

Article

The Differential Effects of Alcohol and Nicotine-Specific Nitrosamine Ketone on White Matter Ultrastructure

A. Papp-Peka¹, M. Tong^{2,3}, J.J. Kril¹, S.M. De La Monte^{2,3}, and G.T. Sutherland^{1,*}

¹Charles Perkins Centre, Discipline of Pathology, School of Medical Sciences, The University of Sydney, Johns Hopkins Drive, Camperdown NSW 2050, Australia, ²Liver Research Center, Department of Medicine, Rhode Island Hospital and the Alpert Medical School of Brown University, Box G-RIH, 55 Claverick Street 4th Floor, Providence, RI 02903, USA, and ³Division of Neuropathology and Departments of Pathology, Neurology, and Neurosurgery, Rhode Island Hospital and the Alpert Medical School of Brown University, USA

*Corresponding author: Discipline of Pathology, Room 6211 Level 6W, Charles Perkins Centre, University of Sydney, Sydney, New South Wales 2006, Australia. Tel: +61 2 90367233; Fax: +61 2 86271601; E-mail: g.sutherland@sydney.edu.au

Received 15 May 2016; Revised 15 August 2016; Accepted 29 August 2016

Abstract

Aims: The chronic consumption of alcohol is known to result in neurodegeneration and impairment of cognitive function. Pathological and neuroimaging studies have confirmed that brain atrophy in alcoholics is mainly due to widespread white matter (WM) loss with neuronal loss restricted to specific regions, such as the prefrontal cortex. Neuroimaging studies of cigarette smokers also suggest that chronic inhalation of tobacco smoke leads to brain atrophy, although the neurotoxic component is unknown. As a high proportion of chronic alcoholics also smoke cigarettes it has been hypothesized that at least some alcohol-related brain damage is due to tobacco smoke exposure.

Methods: 39 Long Evans rats were subjected to 8 weeks exposure to alcohol and/or 5 weeks co-exposure to nicotine-specific nitrosamine ketone (NNK), a proxy for tobacco smoke. Their frontal WM was then assayed with transmission electron microscopy.

Results: NNK and ethanol co-exposure had a synergistic effect in decreasing myelinated fibre density. Furthermore, NNK treatment led to a greater reduction in myelin sheath thickness than ethanol whereas only the ethanol-treated animals showed a decrease in unmyelinated fibre density.

Conclusion: These data suggest that NNK causes WM degeneration, an effect that is exacerbated by alcohol, but unlike alcohol, it has little impact on the neuronal components of the brain.

INTRODUCTION

Alcohol and tobacco are widely used and abused substances that are both high-risk factors for multiple diseases and significant global burdens on healthcare systems. A considerable amount of research demonstrates that alcohol has a degenerative effect on the brain with chronic consumption ultimately leading to alcohol-related brain damage (ARBD), a condition associated with impaired cognitive function including decreased working memory and problem solving ability (Brust, 2010). Early pathological studies of alcoholics found that brain volume reduction was largely

due to loss of white matter (WM) (Sutherland *et al.*, 2014; Harper and Kril, 1985; De la Monte, 1988). Neurodegenerative effects are also seen but, in alcoholics without concomitant thiamine deficiency, these tend to be restricted to the prefrontal cortex (Harper and Kril, 1989; Kril *et al.*, 1997). These findings have been confirmed by neuroimaging studies with the changes being, at least partially, reversible with abstinence (Buhler and Mann, 2011; Pfefferbaum *et al.*, 2014).

Chronic tobacco smoking has been associated with impairments in executive functions (Razani *et al.*, 2004), general intellectual

abilities (Deary *et al.*, 2003), learning and memory (Ernst *et al.*, 2001; Schinka *et al.*, 2003) and cognitive flexibility (Kalmijn *et al.*, 2002). However, unlike ARBD, there is no consensus on the effects on brain atrophy with previous studies reporting increased temporal (Gazdzinski *et al.*, 2005) and cingulate WM volumes (Yu *et al.*, 2011), or no significant change in WM volume (Durazzo *et al.*, 2007; Gallinat *et al.*, 2006; Paul, 2008 #7360). However, decreased WM integrity has been consistently reported (Paul *et al.*, 2008; Zhang *et al.*, 2011). Furthermore, it is unclear what component(s) of tobacco smoke might be responsible. There are more than 4000 toxic compounds in tobacco smoke including carbon monoxide, aldehydes and dihydroxybenzenes. There are also several kinds of tobacco specific nitrosamines, of which 4-(methylnitrosamino)-1-(3-pyridyl)-1-butanone (also known as nicotine-specific nitrosamine ketone (NNK)) is the most studied. Most studies have focused on NNK's carcinogenic effects but sub-mutagenic doses (2 mg/kg), that are known to be hepatotoxic (Zabala *et al.*, 2015), may also have neurodegenerative effects, as seen with other nitrosamines such as streptozotocin (Lester-Coll *et al.*, 2006).

ARBD is likely to result from a variable interaction between the direct and indirect effects of alcohol on the brain combined with co-substance abuse, malnutrition, head trauma and systemic disease. It has been estimated that more than 80% of chronic alcoholics regularly smoke tobacco (Kalman *et al.*, 2005) and recent neuroimaging studies have suggested that a proportion of the damage seen in ARBD is due to smoking (Gazdzinski *et al.*, 2005; Luhar *et al.*, 2013; Durazzo *et al.*, 2014). To date, there has been only one pathological study looking at how chronic tobacco smoking affects the human brain (McCorkindale *et al.*, 2016).

Experimental models of chronic alcohol and smoking behaviour, where there is strict control of dose and elimination of confounding variables, allow direct effects to be measured more accurately. De La Monte and colleagues have developed a rat model of chronic/binge alcohol and NNK consumption (Zabala *et al.*, 2015). They have recently used this model to show that oligodendroglial gene and protein expression is perturbed by co-exposure and that this likely leads to impaired myelin synthesis (Tong *et al.*, 2015b). Here, we extend this work by using transmission electron microscopy (TEM) to investigate whether myelin ultrastructure is affected in these rats and the relative effects of alcohol versus NNK.

METHODS

All animal experiments were carried out at The Rhode Island Hospital-Alpert Medical School of Brown University following approval the Institutional Animal Care and Use committee at the Lifespan-Rhode Island Hospital, and conformed to the National Institute of Health (NIH) guidelines. The Animal Ethics Committee (AEC) of University of Sydney approved the subsequent use of brain tissue samples.

The alcohol/NNK model used here has been previously published (Zabala *et al.*, 2015) and this study is part of a larger programme to examine the combined effects of alcohol and NNK on liver (Zabala *et al.*, 2015) and brain function (Tong *et al.*, 2015a, b). Briefly, 39 1-month-old (adolescent) Long Evans (male) rats were administered isocaloric liquid diets containing 0% or 26% ethanol (alcohol) by caloric content (0% or 6% v/v) for a period of 2 months (8 weeks). The liquid diets were refreshed daily and as this was not a behaviour-based alcohol consumption experiment the rats did not have a choice between ethanol-containing and ethanol-free diets.

Residual food was measured at 10 am each day to monitor food intake. To ensure equivalent caloric intake, the volumes of liquid diet supplied were balanced based on inter-group differences in the amounts consumed, although both groups consumed all of the food supplied each day. From Week 3 until Week 8, rats in each group ($n = 9$ or 10) were administered intraperitoneal NNK (2 mg/kg) or saline on Mondays, Wednesdays and Fridays. In Weeks 7 and 8, ethanol-treated rats were binged with 2 g/kg ethanol (100 μ l, intraperitoneal) on Tuesdays, Thursdays and Saturdays or saline for the controls. Binge administration of ethanol increased the blood alcohol concentrations (BACs) by 2- to 4-fold (mean 70 mg dl⁻¹ chronic to 240, albeit this was slightly lower with NNK + ethanol treatment (200 mg dl⁻¹) (Zabala *et al.*, 2015)). The rats were euthanized with isoflurane and exsanguinated by cardiac puncture. Their frontal lobes were dissected out and a representative WM tissue block removed and fixed by immersion in modified Karnovsky's fixative (2.5% glutaraldehyde and 2% paraformaldehyde in 0.15 M sodium cacodylate buffer) for TEM. Tissue samples were washed and post-fixed in 1% osmium tetroxide (OsO₄), dehydrated in increasing concentrations of acetone and embedded in Spurr's epoxy resin for sectioning. Three ultrathin sections (70 nm) were obtained from each block and placed on copper mesh grids. Sections were subsequently stained with dilute uranyl acetate and lead citrate. All sections were examined on a JEM 1400 transmission electron microscope (JEOL Ltd, Tokyo, Japan) at 120 kV at Sydney Microscopy and Microanalysis, University of Sydney. All TEM images were captured using a high-resolution Gatan digital CCD camera (Gatan, Pleasanton, CA, United States) and imported into open source GIMP (version 2.9.1, www.gimp.org) for adjustment of contrast and Image J (version 1.50b, wsr.nih.gov) for quantitation. TEM images were obtained in a random but systematic fashion. The field of view in the top left part of the section and a series of fields imaged by moving in a clockwise direction at random intervals. The accuracy of fibre counts was determined using a count-recount process on selected images from the control group. Otherwise the rater was blind to group status.

Myelinated fibre density

Low magnification (3000 \times) images were imported into Image J. Images were divided into six equal square areas and an unbiased counting frame (100 μ m²) placed in the centre of each square. Each image was then examined in a systematic and uniform manner using a cell counter application in Image J. Myelinated fibres were counted if they were inside the counting frame, touching an inclusion line, were round or elliptical in cross section and free of artefacts such as sheath unravelling (Fig. 1A). For each section the myelinated fibres were counted in five TEM fields (1140 μ m² per field, at 3000 \times) of three sections per rat (15 images per rat, approximately 150 images per treatment group) and standardized to the mean number of myelinated fibres per 100 μ m².

Myelinated fibre diameter

High magnification (30,000 \times) images were imported into Image J and the diameter of 10 randomly chosen myelinated fibres measured from three sections per rat. Fibres were also classified as small, medium and large as previously described (Liu and Schumann, 2014) and based on the fibre size distribution of the controls only (Fig. 1A).

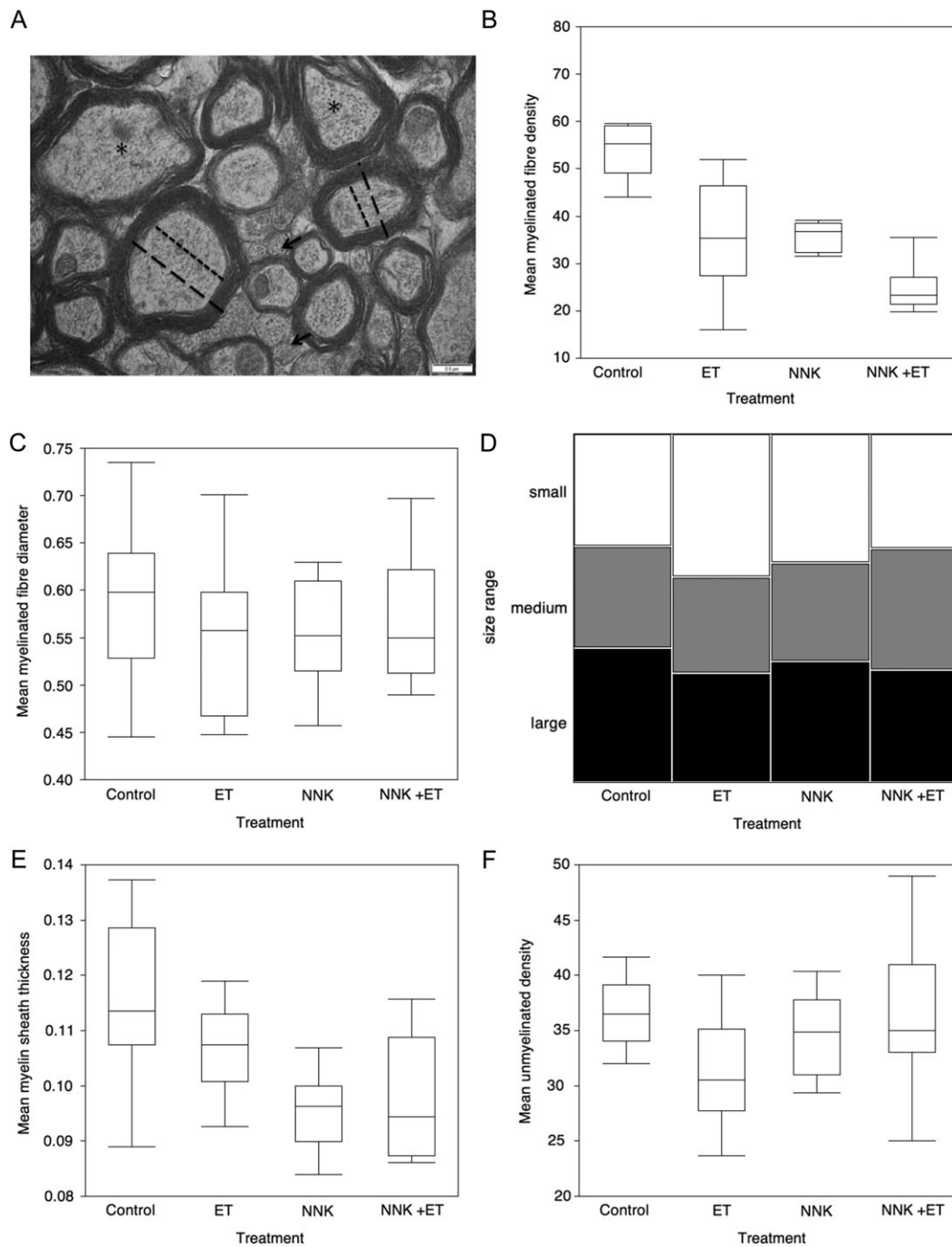


Fig. 1. Quantification of WM integrity. The integrity of fibres in the frontal lobe WM of Long Evans rats were collectively measured using four indices: (A) A high-resolution electron micrograph shows the features measured to derive the four indices. Myelinated and unmyelinated (black arrows) fibres were enumerated in 3000x and 15,000x magnified digital images, respectively. The diameter of those myelinated fibres (long dashed lines) in, or approximately in, cross section were measured using the image analysis software, Image J. Myelin sheath thickness was calculated by subtracting the axon diameter (short dashed lines) from the fibre diameter and dividing the difference by two. Myelinated fibres that were not in cross section (asterisks) were excluded from the analysis. Scale bar 0.5 μ m. Box plots demonstrate the effect of ethanol (ET), NNK and NNK + ethanol on (B) mean myelinated fibre density and (C) mean myelinated fibre diameter. Each plot represents the mean data from 10 rats (or 9 in the combined treatment group) while the box itself shows the median and 75% and 25% quartiles. The whiskers define data that fall within the following range: third quartile + 1.5*(interquartile range) and first quartile - 1.5*(interquartile range). (D) A mosaic histogram shows the distribution of small ($\leq 0.42 \mu$ m, white), medium ($> 0.42 \leq 0.6 \mu$ m, grey) and large ($> 0.6 \mu$ m, black) myelinated fibres in the ethanol (ET)-, NNK-, co-treated and control groups. All graphs were generated with JMP version. 10.0.0. Box plots demonstrate (E) myelin sheath diameter and (F) unmyelinated fibre diameter.

Myelin sheath thickness

High magnification (30,000 \times) images were imported into Image J and the diameter of the axon and whole fibre measured and sheath thickness calculated. Ten myelinated fibres were counted per section, 30 per rat. Myelinated fibres that had unravelled or disrupted sheaths were excluded (Fig. 1A).

Unmyelinated fibre density

The density of unmyelinated fibres was obtained in a similar fashion to myelinated fibre density but from mid-range magnification (15,000 \times) images for accurate visualization. Furthermore fibres quantified across the whole field rather than within unbiased counting frames. Five fields were counted in three sections, 15 per rat. All counts were standardized to unmyelinated fibres per 100 μm^2 .

Statistical analysis

Statistical analyses were performed using the JMP PRO statistical software program (Version 9.0.0, SAS Institute, Cary, North Carolina, USA). The distribution of data was determined with goodness of fit tests (Shapiro–Wilk). For each index differences were assessed using analysis of variance (ANOVA). Post-hoc analysis between individual groups assessed using ANOVA or non-parametric testing (Wilcoxon) if data were not normally distributed. A Chi-squared test was used to assess potential differences in fibre size classes (small, medium and large). Data are reported as mean per treatment \pm standard deviation and results of post-hoc analyses considered statistically significant at an adjusted α -level of 0.02 to allow for multiple comparisons.

RESULTS

A total of 39 Long Evans rats underwent experimental paradigms simulating the chronic/binge pattern of alcohol drinking behaviour (Naimi *et al.*, 2003; Seth *et al.*, 2011) and comorbid smoking (Kalman *et al.*, 2005). Long Evans rats are particularly susceptible to the effects of ethanol on the liver (Yeon *et al.*, 2003; Denucci *et al.*, 2010) and brain (Miura *et al.*, 2008; de la Monte *et al.*, 2009). Intraperitoneal administration of ethanol increases the likelihood of oxidative damage compared with oral gavage (Nogales *et al.*, 2014). NNK was chosen as a proxy for tobacco smoke exposure as it is the prominent nitrosamine in tobacco smoke and other nitrosamines such as streptozotocin (Lester-Coll *et al.*, 2006; Ghosh *et al.*, 2009) are known to be neurotoxic. In this model, BAC increased 4-fold from a mean of 70–240 mg dl⁻¹ following binge doses, although maximum BAC was slightly lower with combined NNK treatment (200 mg dl⁻¹) (Zabala *et al.*, 2015). The rats were divided into subgroups composed of 10 controls, 10 NNK-treated, 10 ethanol-treated and nine NNK + ethanol-treated and four WM integrity indices measured on digital TEM images: myelinated fibre density, unmyelinated fibre density, myelinated fibre size and sheath thickness.

Myelinated fibre density

There was a significant difference in mean myelinated fibre density between the four groups ($P < 0.0001$) with independent effects of ethanol ($P < 0.0001$) and NNK ($P < 0.0001$) along with an interaction between the two treatments ($P < 0.0004$) (Figs 1B and 2). In comparison to the control group (55.6 \pm 9.4, per 100 μm^2), there was a 35% decrease in myelinated fibre density in ethanol-treated

rats (36.3 \pm 12.0, per 100 μm^2 ; $P < 0.0001$), a 36% decrease in NNK-treated rats (35.7 \pm 3.2, per 100 μm^2 ; $P < 0.0001$) and a 44% decrease in the rats exposed to both NNK and ethanol (24.6 \pm 4.8, per 100 μm^2 ; $P < 0.0001$). The combined treatment group had significantly fewer myelinated fibres than either treatment group alone ($P < 0.004$ and $P < 0.006$). There was no difference between the NNK and ethanol-treated groups.

Myelinated fibre diameter

There were no differences in mean fibre diameter between the four groups (Fig. 1C). There were also no group differences in fibre size classes (small, medium and large; $P = 0.14$), although the percentage of large fibres was lowest in the ethanol-treated group (14%, $P = 0.06$) compared with controls (19%), NNK-treated (16%) and co-treated animals (16%) (Fig. 1D).

Myelin sheath thickness

There was a difference in myelin sheath thickness between the four groups ($P = 0.004$) with pairwise analyses showed thinning in NNK-treated groups (both -17% ; $P = 0.0001$ and $P = 0.0008$ (combined)) compared to controls (Fig. 1E). The NNK-treated group was also significantly thinner than the ethanol-treated group ($P = 0.02$) that was, in turn, similar to the control group (-8% , $P = 0.07$).

Unmyelinated fibre density

As unmyelinated fibres without an electron dense sheath were more difficult to discern in TEM micrographs they were quantified in 15,000 \times images (15 per rat) or approximately 5-fold less sampling, by area, than for myelinated fibres. There was a significant difference in unmyelinated fibre density between the treatment groups ($P = 0.003$) (Fig. 1F). Pairwise analyses showed that only ethanol-treated animals significantly differed from controls ($P = 0.01$). A two-way ANOVA revealed an interaction of NNK and ethanol ($P = 0.001$) with co-exposed animals demonstrating the smallest reduction in unmyelinated fibres (2%) compared to NNK- (8%) and ethanol-treated animals (16%).

DISCUSSION

This study examined the effect of chronic alcohol and NNK exposure on frontal lobe WM integrity in male Long Evans rats at an ultrastructural level. The results suggest a synergistic effect between the two exposures on myelinated fibre density but more complex interactions with other WM indices. In particular, the tobacco smoke component, NNK, appeared to specifically target the myelin sheath while the majority of ethanol's effects appear to be directed at the axonal (neuronal) component of WM.

Is NNK neurodegenerative?

In the narrow sense of the term, NNK may not be neurodegenerative as its effects on WM appear to be confined to myelin integrity. Assuming that NNK is a reasonable proxy for tobacco smoke, then the findings here are consistent with human neuroimaging studies that showed smoking had an adverse effect on WM, and in particular decreased frontal lobe WM integrity (Zhang *et al.*, 2011). Furthermore, these results are consistent with studies that demonstrated that smoking leads to impaired cognitive function (Durazzo *et al.*, 2007; Deary *et al.*, 2003; Gazdzinski *et al.*, 2005).

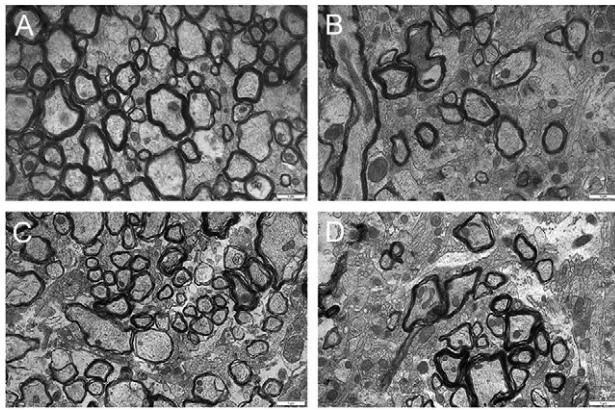


Fig. 2. The effects of ethanol and NNK treatment on WM. Representative high-resolution transmission electron micrographs show WM in the frontal lobe of a Long Evans rat from the (A) control group, (B) ethanol-treated group, (C) NNK-treated group and (D) combined ethanol and NNK-treated group. These 15,000 \times images are not necessarily consistent with the 3000 \times images used to derive mean myelinated fibre densities. Scale bars 1 μ m.

Ethanol

There seemed to be a subtle difference in the mechanism of action of ethanol versus NNK on the rat brain. Ethanol had no effect on myelin sheath thickness but had a similar effect to NNK on myelinated fibre density. In contrast ethanol was the only treatment to affect unmyelinated fibre density. Notwithstanding there was less sampling of unmyelinated fibres in the study, it does appear that ethanol, but not NNK, is directly neurotoxic. These results are consistent with the widespread WM loss seen in ARBD (de la Monte, 1988; Kril *et al.*, 1997; Sutherland *et al.*, 2014). In the absence of TEM studies on ARBD the effect of ethanol on unmyelinated fibres appears consistent with the moderate but localized GM atrophy and neuronal loss seen in areas such as the prefrontal cortex (Harper and Kril, 1989; Kril *et al.*, 1997).

Interactive effects between ethanol and NNK

The deleterious effect of ethanol and NNK on myelinated fibres may represent a double hit on the neuronal and oligodendroglial (myelin) components, respectively, of the myelinated fibres. Whereas the disparate effects on unmyelinated fibres suggest that in the absence of myelin, NNK can attenuate ethanol neurotoxicity. These results are generally consistent with neuroimaging studies. A MRI study by Gazdzinski *et al.* (2005) found significant GM losses in the temporal, parietal and occipital lobes in alcoholics (Gazdzinski *et al.*, 2005). When this group re-analysed their results they found that these reductions were largely found in smoking alcoholics compared rather than non-smoking alcoholics (Durazzo *et al.*, 2007). These findings, along with greater WM loss also in smoking alcoholics, have since been replicated (Luhar *et al.*, 2013; Durazzo *et al.*, 2014). In terms of a sparing effect of smoking on neuronal damage, our own work using autopsy tissue suggested trends towards increased volume in smokers in two GM regions (the supramarginal and sensory cortex) but there was no correlation to smoking pack-years (McCorkindale *et al.*, 2016).

Potential mechanisms

The findings here support a synergistic effect, although not strictly additive, of ethanol and NNK on WM injury in this rat model.

These findings are consistent with those of De La Monte and colleagues who demonstrated with light microscopy in the same tissue that NNK and ethanol combined caused the loss of myelinated fibres and impaired memory and spatial learning (Tong *et al.*, 2015b). Tong *et al.* did observe a greater effect of ethanol on myelin sheath thickness than observed here. They also showed that the combined exposures decreased the expression proteins such as myelin-associated glycoprotein, proteolipid protein 1 and myelin basic protein in mature oligodendrocytes. Whereas there was increased expression of immature oligodendroglial genes such as platelet-derived growth factor receptor, alpha polypeptide. Interestingly, ethanol blocked these inhibitory effects. Tong *et al.* (2015a) went on to show that sub-mutagenic doses of NNK's neurotoxic effects were associated with the downregulation of the insulin/IGF1 signalling pathway and increased oxidative damage although not to the same degree as seen with ethanol alone.

Other TEM studies

Our study was a novel exploration of the combined effects of smoking and chronic alcohol consumption on WM ultrastructure in rats. The control group can be directly compared to previous TEM studies in rats that have looked at the effects of ageing (Li *et al.*, 2008; Yang *et al.*, 2009), malnutrition (Olivares *et al.*, 2012) and alcohol/thiamine deficiency (He *et al.*, 2006). Yang *et al.* (2009) reported that myelinated fibre diameter in cortical WM increased with age and that the youngest female Long Evans rats (6 months) had a mean diameter of 0.56 μ m, the same figure observed here. In contrast, Olivares *et al.* (2012) quantified myelinated fibres in the corpus callosum of 6-week-old Sprague-Dawley rats and found a mean diameter of 0.49 μ m. In terms of myelin sheath thickness the current mean (0.12 μ m in controls) is consistent with the mean thickness in two previous studies of 0.13 μ m (He *et al.*, 2006) and 0.12 μ m (Li *et al.*, 2008).

In particular He *et al.* (2007) looked at the interaction between alcohol and thiamine deficiency on myelin fibres in the corpus callosum of 18-months male Wistar alcohol-preferring rats. They found that the alcohol/thiamine deficient (pyrithamine) group had smaller fibres, lower myelinated fibre diameter, thinner myelin sheaths but greater myelinated fibre density. There were interactions between alcohol and thiamine deficiency but the latter was largely responsible for WM damage seen. He *et al.* suggested that a selective loss or shrinkage of large fibres was responsible for the increase in myelinated fibre density. The more subtle alcohol effects reported by He *et al.* may reflect the chronic, intermittent exposure over 12 months, the strain and the age of the rats. Interestingly, a previous TEM study in human postmortem tissue of chronic alcoholics also failed to show a difference in WM volume or myelinated fibre diameter (Tang *et al.*, 2004). However, Tang *et al.* did note a non-significant reduction (9%) subcortical WM in alcoholics, similar to the 11% reduction in total WM seen in a previous volumetric study by their group (Jensen and Pakkenberg, 1993) and the 12% reduction in total WM reported recently by our group (McCorkindale *et al.*, 2016).

CONCLUSION

This study provides evidence that NNK and ethanol have a synergistic relationship that results in WM degeneration. NNK and ethanol had similar effects on most of the indices measured suggesting that their pathomechanisms overlap to some degree but NNK had a greater effect on myelin integrity while ethanol had additional

axonal effects. Further work is required to determine whether these findings can be extrapolated to ultrastructural studies of post-mortem tissue from smoking and non-smoking alcoholics.

ACKNOWLEDGEMENTS

The authors would like to thank Drs Naveena Gokoolparsadh, Hongwei Liu and Matthew Foley at Sydney Microscopy and Microanalysis (University of Sydney) for their assistance with TEM and image analysis.

FUNDING

This study was supported by R28 AA012725, AA-11431, AA-12908 and Diversity supplement to AA-11431 from the National Institutes of Health.

CONFLICT OF INTEREST STATEMENT

None declared.

REFERENCES

- Brust JC. (2010) Ethanol and cognition: indirect effects, neurotoxicity and neuroprotection: a review. *Int J Environ Res Public Health* 7:1540–57.
- Buhler M, Mann K. (2011) Alcohol and the human brain: a systematic review of different neuroimaging methods. *Alcohol Clin Exp Res* 35:1771–93.
- de la Monte SM. (1988) Disproportionate atrophy of cerebral white matter in chronic alcoholics. *Arch Neurol* 45:990–2.
- de la Monte SM, Tong M, Lawton M, et al. (2009) Nitrosamine exposure exacerbates high fat diet-mediated type 2 diabetes mellitus, non-alcoholic steatohepatitis, and neurodegeneration with cognitive impairment. *Mol Neurodegener* 4:54.
- Deary IJ, Pattie A, Taylor MD, Whiteman MC, Starr JM, Whalley LJ. (2003) Smoking and cognitive change from age 11 to age 80. *J Neurol Neurosurg Psychiatry* 74:1006–07.
- Denucci SM, Tong M, Longato L, et al. (2010) Rat strain differences in susceptibility to alcohol-induced chronic liver injury and hepatic insulin resistance. *Gastroenterol Res Pract*. doi:10.1155/2010/312790.
- Durazzo TC, Cardenas VA, Studholme C, et al. (2007) Non-treatment-seeking heavy drinkers: effects of chronic cigarette smoking on brain structure. *Drug Alcohol Depend* 87:76–82.
- Durazzo TC, Mon A, Pennington D, et al. (2014) Interactive effects of chronic cigarette smoking and age on brain volumes in controls and alcohol-dependent individuals in early abstinence. *Addict Biol* 19:132–43.
- Ernst M, Heishman SJ, Spurgeon L, London ED. (2001) Smoking history and nicotine effects on cognitive performance. *Neuropsychopharmacology* 25: 313–19.
- Gallinat J, Meisenzahl E, Jacobsen LK, et al. (2006) Smoking and structural brain deficits: a volumetric MR investigation. *Eur J Neurosci* 24: 1744–50.
- Gazdzinski S, Durazzo TC, Studholme C, et al. (2005) Quantitative brain MRI in alcohol dependence: preliminary evidence for effects of concurrent chronic cigarette smoking on regional brain volumes. *Alcohol Clin Exp Res* 29:1484–95.
- Ghosh D, Mishra MK, Das S, et al. (2009) Tobacco carcinogen induces microglial activation and subsequent neuronal damage. *J Neurochem* 110:1070–81.
- Harper C, Kril J. (1985) Brain atrophy in chronic alcoholic patients: a quantitative pathological study. *J Neurol Neurosurg Psychiatry* 48:211–7.
- Harper C, Kril J. (1989) Patterns of neuronal loss in the cerebral cortex in chronic alcoholic patients. *J Neurol Sci* 92:81–9.
- He X, Sullivan EV, Stankovic RK, et al. (2007) Interaction of thiamine deficiency and voluntary alcohol consumption disrupts rat corpus callosum ultrastructure. *Neuropsychopharmacology* 32:2207–16.
- He XH, Pfefferbaum A, Sullivan EV, et al. (2006) A quantitative morphometric analysis of myelinated fibres in corpus callosum following thiamine deficiency and alcohol exposure in the alcohol-preferring (P) rat. *Alcohol Clin Exp Res* 30:159A.
- Jensen GB, Pakkenberg B. (1993) Do alcoholics drink their neurons away? *Lancet* 342:1201–4.
- Kalman D, Morissette SB, George TP. (2005) Co-morbidity of smoking in patients with psychiatric and substance use disorders. *Am J Addict* 14: 106–23.
- Kalmijn S, van Boxtel MP, Verschuren MW, Jolles J, Launer LJ. (2002) Cigarette smoking and alcohol consumption in relation to cognitive performance in middle age. *Am J Epidemiol* 156:936–44.
- Kril JJ, Halliday GM, Svoboda MD, et al. (1997) The cerebral cortex is damaged in chronic alcoholics. *Neuroscience* 79:983–98.
- Lester-Coll N, Rivera EJ, Soscia SJ, et al. (2006) Intracerebral streptozotocin model of type 3 diabetes: relevance to sporadic Alzheimer's disease. *J Alzheimers Dis* 9:13–33.
- Li C, Yang S, Zhang W, et al. (2008) Unbiased stereological quantification of unmyelinated fibers in the rat brain white matter. *Neurosci Lett* 437: 38–41.
- Liu XB, Schumann CM. (2014) Optimization of electron microscopy for human brains with long-term fixation and fixed-frozen sections. *Acta neuropathol communit* 2:42.
- Luhar RB, Sawyer KS, Gravitz Z, et al. (2013) Brain volumes and neuropsychological performance are related to current smoking and alcoholism history. *Neuropsychiatr Dis Treat* 9:1767–84.
- McCorkindale A, Sheedy D, Kril JJ, et al. (2016) The effects of chronic smoking on the pathology of alcohol-related brain damage. *Alcohol* 2016 Jun 53:35–44.
- Miura TA, Travanty EA, Oko L, et al. (2008) The spike glycoprotein of murine coronavirus MHV-JHM mediates receptor-independent infection and spread in the central nervous systems of Ceacam1a-/- Mice. *J Virol* 82: 755–63.
- Naimi TS, Brewer RD, Mokdad A, et al. (2003) Binge drinking among US adults. *JAMA* 289:70–5.
- Nogales F, Rua RM, Ojeda ML, et al. (2014) Oral or intraperitoneal binge drinking and oxidative balance in adolescent rats. *Chem Res Toxicol* 27: 1926–33.
- Oliveiras R, Morgan C, Perez H, et al. (2012) Anatomy of corpus callosum in prenatally malnourished rats. *Biol Res* 45:87–92.
- Paul RH, Grieve SM, Niaura R, et al. (2008) Chronic cigarette smoking and the microstructural integrity of white matter in healthy adults: a diffusion tensor imaging study. *Nicotine Tob Res* 10:137–47.
- Pfefferbaum A, Rosenbloom MJ, Chu W, et al. (2014) White matter microstructural recovery with abstinence and decline with relapse in alcohol dependence interacts with normal ageing: a controlled longitudinal DTI study. *Lancet Psychiatry* 1:202–12.
- Razani J, Boone K, Lesser I, Weiss D. (2004) Effects of cigarette smoking history on cognitive functioning in healthy older adults. *Am J Geriatr Psychiatry* 12:404–11.
- Schinka JA, Belanger H, Mortimer JA, Graves AB. (2003) Effects of the use of alcohol and cigarettes on cognition in elderly African American adults. *J Int Neuropsychol Soc* 9:690–97.
- Seth D, Haber PS, Syn WK, et al. (2011) Pathogenesis of alcohol-induced liver disease: classical concepts and recent advances. *J Gastroenterol Hepatol* 26:1089–105.
- Sutherland GT, Sheedy D, Kril JJ. (2014) Neuropathology of alcoholism. In: Vinken PJ, Bruyn GW (eds), *Handbook of Clinical Neurology*. NX Amsterdam, The Netherlands: Elsevier, Vol. (125):603–15.
- Tang Y, Pakkenberg B, Nyengaard JR. (2004) Myelinated nerve fibres in the subcortical white matter of cerebral hemispheres are preserved in alcoholic subjects. *Brain Res* 1029:162–7.
- Tong M, Yu R, Deochand C, et al. (2015a) Differential contributions of alcohol and the nicotine-derived nitrosamine ketone (NNK) to insulin and insulin-like growth factor resistance in the adolescent rat brain. *Alcohol Alcohol* 50:670–9.
- Tong M, Yu R, Silbermann E, et al. (2015b) Differential contributions of alcohol and nicotine-derived nitrosamine ketone (nnk) to white matter pathology in the adolescent rat brain. *Alcohol Alcohol* 50:680–9.

- Yang S, Li C, Lu W, *et al.* (2009) The myelinated fiber changes in the white matter of aged female Long-Evans rats. *J Neurosci Res* 87:1582–90.
- Yeon JE, Califano S, Xu J, *et al.* (2003) Potential role of PTEN phosphatase in ethanol-impaired survival signaling in the liver. *Hepatology* 38:703–14.
- Yu R, Zhao L, Lu L. (2011) Regional grey and white matter changes in heavy male smokers. *PLoS One* 6:e27440.
- Zabala V, Tong M, Yu R, *et al.* (2015) Potential contributions of the tobacco nicotine-derived nitrosamine ketone (nnk) in the pathogenesis of steatohepatitis in a chronic plus binge rat model of alcoholic liver disease. *Alcohol Alcohol* 50:118–31.
- Zhang X, Salmeron BJ, Ross TJ, *et al.* (2011) Factors underlying prefrontal and insula structural alterations in smokers. *Neuroimage* 54:42–8.